6 Imaging Modalities and Characteristics in Medication-Related Osteonecrosis of the Jaw

Florian A. Probst, Monika Probst, and Sotirios Bisdas

Abstract

Though diagnosis itself is based on anamnesis and clinical presentation, imaging occupies an integral part of the management of medication-related osteonecrosis of the jaws (MRONJ). Various radiographic signs may be seen on panoramic radiographs, cone-beam computed tomography (CBCT), or multislice CT (MSCT) like sclerosis, persisting alveolar sockets, and lack of bone filling in extractions sites, osteolysis, and sequestration. While panoramic radiographs serve as a baseline diagnostic tool, computed tomography (CT) or cone-beam computed tomography (CBCT) and magnetic resonance imaging (MRI) provide three-dimensional information of osteonecrotic lesions and may aid in assessing the extent of necrosis, monitoring the disease, and detecting early lesions. Anyway, no imaging modality is able to reliably depict the margins of a necrosis so far. CT and MRI offer a wide spectrum of findings but those are often not very specific. In the future, nuclear medicine imaging like combined SPECT/CT or PET/CT may further improve the diagnosis of MRONJ by combining functional and anatomical information.

F.A. Probst, MD, DDS (✉)
Department of Oral and Maxillofacial Surgery, University Hospital Munich (LMU), Lindwurmstr. 2a, Munich 80337, Germany
e-mail: florian.probst@med.uni-muenchen.de

M. Probst, MD
Department of Neuroradiology, Klinikum rechts der Isar, Technical University Munich, Ismaningerstr. 22, Munich 81675, Germany
e-mail: Monika.probst@tum.de

S. Bisdas, MD, PhD, MSc
Department of Neuroradiology, Eberhard Karls University Tübingen, Hoppe-Seyler-Str. 3, Tübingen 72076, Germany
e-mail: sotirios.bisdas@med.uni-tuebingen.de

Introduction

According to AAOMS criteria and some early reports, the diagnosis of BRONJ is traditionally based on anamnesis and clinical examination [1]. The criteria that have to be fulfilled in order to establish diagnosis of BRONJ are already mentioned in the previous chapters, including clinically exposed bone in the oral cavity for 8 weeks or more [2]. Therefore, imaging techniques are not a prerequisite for the diagnosis itself. However, they play an important role for assessment of the extent of a necrosis and possible side effects

S. Otto (ed.), *Medication-Related Osteonecrosis of the Jaws: Bisphosphonates, Denosumab, and New Agents*,
DOI 10.1007/978-3-662-43733-9_6, © Springer-Verlag Berlin Heidelberg 2015

Table 6.1 Summary of radiographic findings in MRONJ

Radiopacity	Radiolucency	Findings in advanced disease/ complications
Sclerosis, focal/diffuse	Impaired healing of extraction sites, lack of bone filling, persisting alveolar sockets	Sequestra
Thickening of the lamina dura	Osteolysis of cortical/spongious bone	Pathological fractures
Prominent mandibular canal	Focal cortical disruption	Signs of sinusitis
Periosteal reaction	Periradicular lucency	

like accompanying inflammatory soft-tissue involvement or for the detection of pathological fractures. Furthermore, imaging can help to monitor disease progression and to differentiate between osteonecrosis and neoplastic lesion like metastasis. Additionally, imaging is of special interest concerning the detection of early stages of BRONJ, which do not present with clinically exposed bone, corresponding to stage 0 of the disease [3, 4].

While panoramic radiographs serve as valuable basic tools in MRONJ imaging, radiologic tomographic techniques like computed tomography (CT) or cone-beam computed tomography (CBCT) can provide three-dimensional information of the region of interest. Furthermore, magnetic resonance imaging (MRI) is increasingly becoming the focus of attention, as it is assumed that it might aid in early detection and assessment of a lesion's dimension. Last but not least, functional imaging techniques like scintigraphy, bone single-photon emission computed tomography (SPECT), or positron emission tomography with computed tomography (PET/CT) have the potential to complement the radiologic spectrum of MRONJ imaging. In the following, the relevant radiographic, MR, and nuclear medicine imaging techniques for the MRONJ imaging will be pictorially presented.

Panoramic Radiographs

Conventional dentomaxillofacial diagnostic x-ray supplied by periapical and panoramic radiographs allows for baseline MRONJ imaging. Especially panoramic radiographs enable a prompt overview of teeth and mandibular and maxillary bones. They should be considered as an initial imaging modality for patients with suspicion of MRONJ [1, 5, 6]. Panoramic radiographs provide information not only about signs of osteonecrosis but also about coexisting dental aspects like apical osteolysis, periodontal lesions, or carious lesions. Furthermore, plain radiographs are pricy and available in almost every dental clinic and maxillofacial surgery unit.

There are various typical signs of BRONJ on panoramic radiographs (Table 6.1). Alterations of the bone structure may appear mainly with osteolysis, sclerosis, or a combination [6–10]. Sclerosis is a highly frequent sign, seen at all stages of the disease, especially in the early stage [3–5, 11]. Sclerose-like areas can vary from a distinct focal sclerosis of the alveolar process to a diffuse and wide range involvement of greater parts of the mandible or maxilla [3, 11]. Further frequently reported signs are thickening of the alveolar margins, the lamina dura, or the cortical borders and narrowing of the mandibular canal [3, 5, 11, 12]. Also radiolucent appearance with osteolysis, disturbance of the cortical bone, and delayed healing of extraction sockets or even persisting alveolar sockets can be observed (Fig. 6.1) [3, 5, 6, 11, 13]. In advanced stages of BRONJ, sequestra are another typical finding. Moreover, widening of the periodontal ligament space and periapical lucencies may be apparent [11].

Radiologic Tomographic Techniques (CT, CBCT)

In contrast to conventional radiographs, including panoramic radiographs, tomographic techniques like computed tomography (CT) or cone-beam computed tomography (CBCT) allow for three-dimensional evaluation of the jaws.

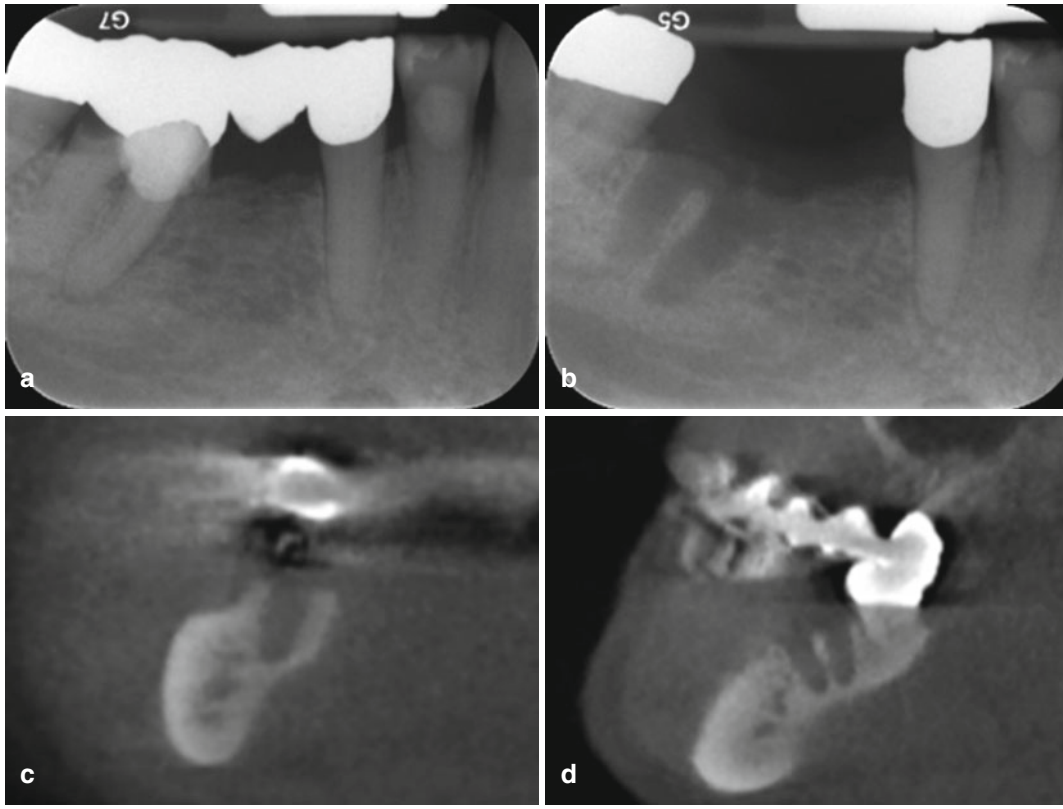

Fig. 6.1 A 70-year-old male presented clinically with a non-healing extraction wound and exposed bone and putrid exudate in the right mandible in region 45–46. Extraction of tooth 46 had been performed 3 months before. The patient received intravenous bisphosphonate therapy with zoledronate (4 mg/month) since 3 and 1/2 years, due to osseous metastases from prostate carcinoma. (**a**) Plain film radiograph prior to extraction. (**b**) Plain film radiograph 3 month after extraction of tooth 46. Lack of bone filling and persisting alveolar sockets are obvious. (**c**) Coronal/(**d**) sagittal sections derived from CBCT data showing lack of bone filling

The radiographic signs of BRONJ on panoramic radiographs, which were described above, can be seen in CT images in an analogous way (Table 6.1).

Based on bisphosphonate-induced disorganized bone homeostasis, the affected bone is often associated with sclerosis [14, 15], and consequently, it is a frequent sign seen in radiologic imaging in BRONJ cases (Table 6.1). Sclerosis can range from focal to extended involvement and may have a flocculent or more dense character with irregular trabeculation (Figs. 6.2, 6.4, and 6.6). In advanced lesions, osteonecrosis can present as an inhomogeneous bone density with "cotton-wool" appearance. Dealing with diffuse sclerosis, buccal and lingual cortical bone was reported to be thickened with reduced contrast to the spongious bone [3]. The mandibular canal can present prominently when sclerosis affects the margins of the canal (Figs. 6.3 and 6.4) [3, 5]. Thickening of the alveolar margins and lamina dura is described as well [3, 5].

On the other side, osteonecrotic areas feature a loss in bone mineralization and fragmentation and often present with radiolucent areas on panoramic radiographs and lowered attenuation in CT (Table 6.1) (Fig. 6.6) [3, 5, 6, 11, 16].

Several reports suggest significant advantages of CT imaging when compared to panoramic radiographs [5, 6, 9, 13, 17–19]. Location and extension of a lesion may be assessed more exactly by tomography. The dimension of a

Fig. 6.2 Multislice computed tomography (MSCT). Extended sclerotic changes of the right mandibular corpus and ramus (*arrowheads*). Sequestration and lingual cortical disruption (*large arrow*)

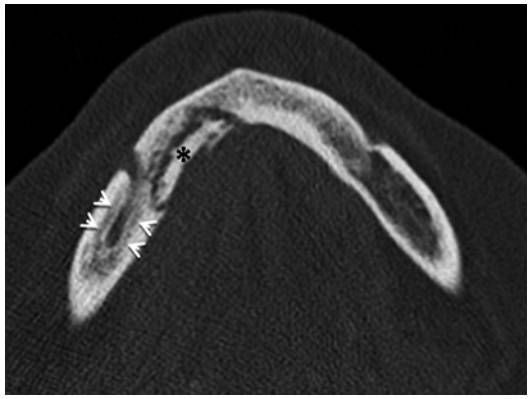

Fig. 6.3 BRONJ in the right mandible. Multislice CT depicting a large lingual mandibular sequestration (*black asterisk*) and prominent mandibular canal (*white arrowheads*) as sclerosis affects the margins of the canal

lesion was proved to be larger on CT and MRI as well as in histopathology than the area of clinically exposed bone [20]. Panoramic radiographs seem to underestimate the dimension of a lesion compared to CT imaging, and the existence of smaller sequestra may be overlooked more easily in panoramic radiographs (Fig. 6.6) [17].

Preoperative knowledge about the extension of a bisphosphonate-related necrosis is valuable for surgical planning. Up to now, there is paucity of available data in this concern. In a study of 24 patients suffering from different stages of

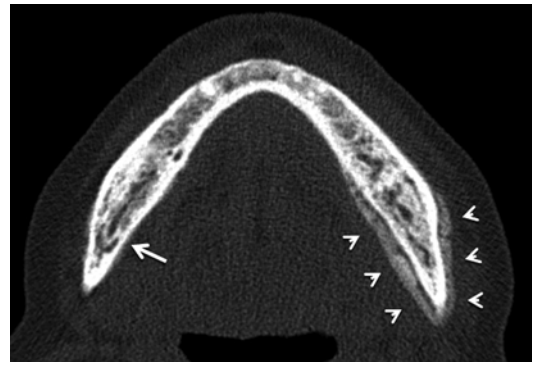

Fig. 6.4 Multislice computed tomography (MSCT). Mandible affected by BRONJ. Extended left perimandibular periosteal reaction (*arrowheads*). Osteosclerosis with disorganized irregular medullary trabeculation throughout the complete mandible. Prominent mandibular canal can be seen at the right mandible (*large arrow*)

BRONJ, panoramic radiographs, CT, and MRI were performed. While detectability of CT and MRI exceeded that of panoramic radiographs by far, it was obvious that CT and MRI presented with difficulties in evaluating the exact extent of the lesions, and so it was concluded that the precision of these both modalities, displaying the extension of osteonecrosis, is limited [9]. Guggenberger et al. (2013) compared extension of bisphosphonate-related lesions in ten patients undergoing PET/CT, contrast-enhanced MRI, panoramic views derived from CBCT, and preoperative and intraoperative assessment. PET/CT and contrast-enhanced MRI were able to display more extensive changes compared with panoramic views derived from CBCT and clinical examination. It was reported that preoperative examination detected smaller extension of the disease than the other examinations. All in all, PET/CT and contrast-enhanced MRI detected more extensive involvement of BRONJ compared with panoramic views from CBCT and clinical examinations [21]. Nonetheless, the latter two studies demonstrate the current limitations of all modalities in order to assess the exact extension of lesion in BRONJ cases. While MRI and PET-CT may overestimate the real lesion dimensions, CBCT imaging as well as preoperative and intraoperative estimations may underestimate the real extension. For the surgeon it is worthwhile to note that for

preoperative work-up, these differences between the imaging modalities should be taken into consideration [21]. Further studies are needed and may include precise histopathological assessment and intraoperative assessment with the aid of fluorescence imaging as described in brief in the treatment chapter [22, 23].

Recently, imaging focus also headed toward the possibility to detect MRONJ in an early stage, when there is no presence of clinically exposed bone in the oral cavity. Sclerosis is reported to be a consistent finding in imaging of early disease [3, 16]. In contrast to low-grade or sclerosing osteomyelitis however, periosteal response seems not to be characteristic in early stages (Fig. 6.4) [3, 10].

In a cohort of 32 patients with BRONJ, a cluster analysis was performed on the basis of different radiologic features. Patients were grouped in 4 categories based on CT findings. The authors found a positive correlation with the clinical extension analysis [17]. In contrast, a staging based solely on panoramic radiographs was judged not to be reliable because lesions tend to be underestimated and because of a missing correlation between clinical extension and dental panoramic radiograph clusters [16]. Purulent secretion and sequestration are correlating with the size of osteonecrotic lesions and demonstrated the value of CT imaging in patients with BRONJ [24].

Quantification of imaging features may be promising in order to assess the presence of a bisphosphonate-related bony disorder in an objective manner. CT imaging and consecutive work-up of bone matrix density were performed in patients with confirmed BRONJ and compared with samples from cadaveric controls. Unfortunately, higher bone tissue density was evident only in a subset of BRONJ patients, suggesting that density may have limitations as a biomarker for early detection of this condition [25].

In a retrospective pilot study, different techniques were tested in order to analyze cortical bone dimensional changes caused by bisphosphonates based on CBCT imaging. The evaluation of the mandibular cortical bone at the site of the mental foramen seems to be helpful for the detection of cortical bone dimensional changes. Alterations in the bone architecture were even evident in areas of the mandible, which were not affected by clinical bone exposure. It was concluded that the technique described may aid in detecting early bone alterations helping to predict BRONJ in individuals. However, further longitudinal studies were proposed to verify this technique [12].

Cone-beam computed tomography (CBCT) is a tomographic imaging technique that has become increasingly popular in dentomaxillofacial imaging over the last decade. Within a short imaging time, high-resolution three-dimensional datasets of the head and neck region can be generated. Software applications allow displaying panoramic views as well as multiplanar reconstructions [26]. Furthermore, CBCT imaging comes along with considerably reduced radiation exposure compared to multislice CT protocols [27, 28]. Accordingly, this technique is of increased importance in the setting of BRONJ [10, 12, 29–33].

Radiographic findings (Table 6.1) can be similarly found in CBCT and multidetector CT (Fig. 6.6). However, it hast to be considered that CBCT attenuation measurements are less reliable compared with those in multidetector CT and soft-tissue contrast is lower compared with multidetector CT [34].

Inflammatory affection of soft tissues like cervical lymphadenopathy, mass-like thickening of the masticator muscles, and abscess formation are addressed more properly with multidetector CT imaging or MRI, especially if imaging is contrast enhanced.

Further radiographic findings in advanced disease that should be kept in mind are sequestra, pathological fractures, and maxillary sinus affection (Figs. 6.2, 6.3, 6.5, and 6.6) [35, 36]. These findings should be given special attention and three-dimensional imaging modalities are strongly recommended in this context. For example, panoramic radiographs seem to underestimate the dimension of a lesion compared to CT imaging, and the existence of smaller sequestra may be overlooked more easily in panoramic radiographs (Fig. 6.6) [17, 35].

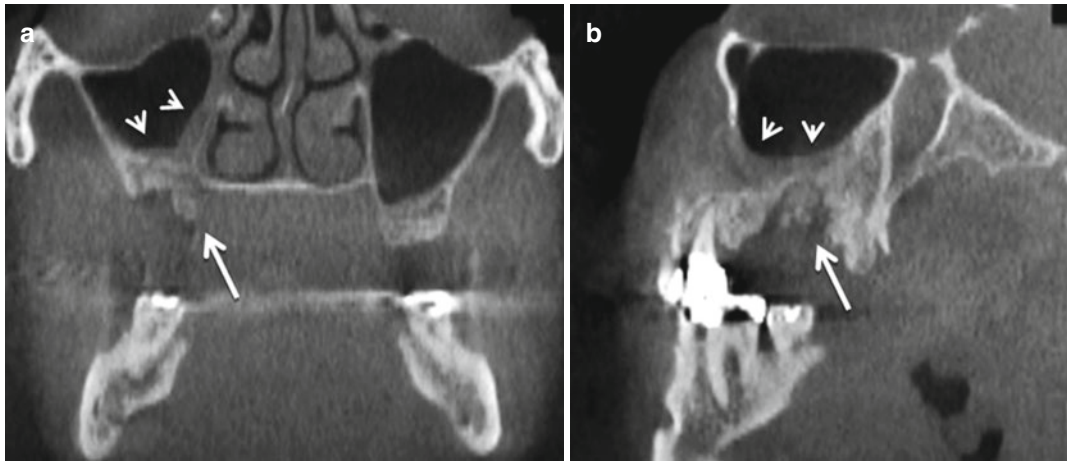

Fig. 6.5 A 73-year-old male clinically presenting with signs of sinusitis and exposed bone in the right posterior maxilla. (**a**) Coronal and (**b**) sagittal sections derived from CBCT data. *Large arrows* are depicting a sequestrum. *Arrowheads* show mucosal thickening in the right maxillary sinus as radiologic correlate to maxillary sinusitis due to BRONJ

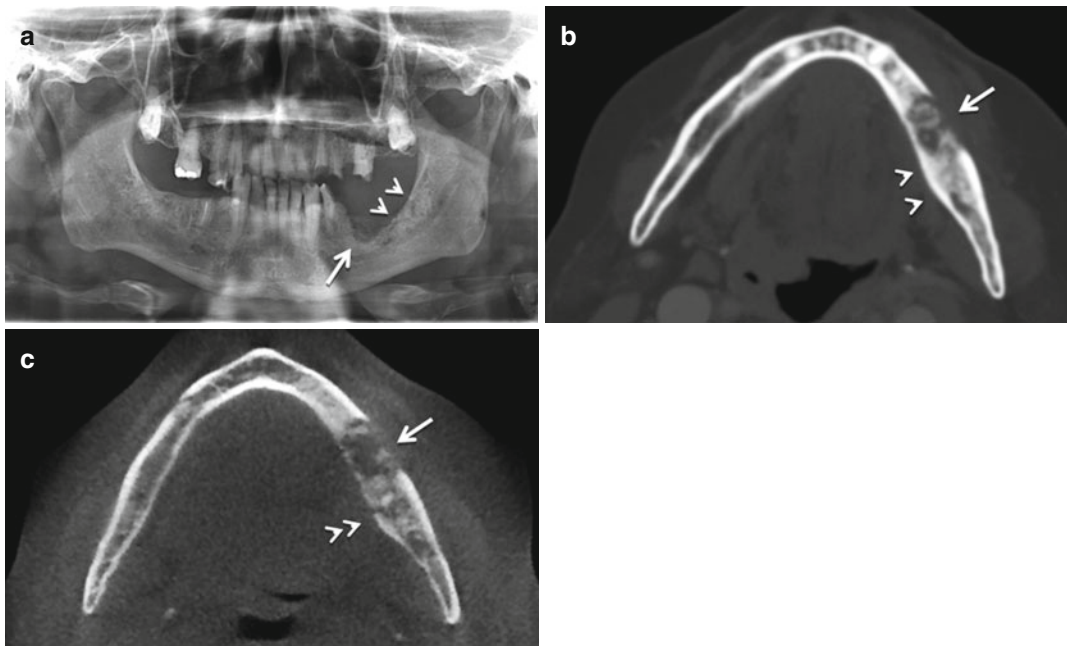

Fig. 6.6 A 69-year-old male patient received intravenous bisphosphonate therapy with zoledronate (4 mg/month) due to osseous metastases from prostate carcinoma. (**a**) Panoramic radiograph. *Large arrow* is showing a radiolucent area corresponding to alveolar margin osteolysis. Posterior to the osteolysis, the *two arrowheads* depict osteosclerosis with disorganized medullary trabeculation and "cotton-wool"-like appearance. (**b**) Multislice computed tomography (MSCT). The *large arrow* indicates the osteolytic area; the *two arrowheads* indicate the osteosclerosis. In contrast to the panoramic radiograph, sequestration is visible as well (within the osteolytic area). (**c**) Cone-beam computed tomography (CBCT). Osteolytic area can be seen as well (*large arrow*). Additionally, lingual cortical disruption becomes evident in the shown layer (*consecutive arrowheads*)

Magnetic Resonance Imaging (MRI)

Free from ionizing radiation, MR imaging should be preferentially performed in 1.5 T or 3 T MR units, which may use the full spectrum of the modern sequences that provide "state-of-the-art" 2D and 3D T1- and T2-weighted imaging [9, 16, 21]. New MR scanners are also offered with multiple channel head/neck coils (up to 32 channels) that enable superior spatial resolution (in submillimeter range) in reasonable acquisition time for the patient. Besides the conventional morphological imaging, which has to be enhanced by contrast agent administration and suitable saturation of the fat planes in extracranial head, new functional MR imaging techniques (i.e., perfusion, diffusion) are available and may facilitate early disease diagnosis or monitoring in the future. Nonetheless, preliminary studies failed to demonstrate any strong supporting evidence in clinically manifested cases [37] as well as in the early stage of non-traumatic osteonecrosis models [38].

MR imaging of BRONJ is complementary to CT imaging revealing signal intensity alterations in a homogeneous pattern or affecting the periphery of the lesion in a band-like pattern [16], which has also a close correlation to the "bone-within-bone" appearance often seen in CT [16, 39]. In general, BRONJ is typically associated with decreased signal intensity on T1-weighted images and variable signal intensity changes on T2-weighted or short inversion time inversion-recovery (STIR) images and contrast-enhanced images [6, 7, 16, 40]. Typically, low T1 signal (reflecting low water content) in open wounds is associated with intermediate or slightly increased signal intensity on T2-weighted images (reflecting edema and inflammation) (Figs. 6.7, 6.8, and 6.9). Rather than T1-weighted images, the T2 signal intensity of the abnormalities, possibly associated with the disease stage including early cases with intermediate symptoms, is not variable, thus not pathognomonic and should be meticulously appreciated together with the CT findings, which may reveal subtle changes (i.e., focal hyperdensity) [6, 16, 40]. Generally, little information has been published about the early stages of BRONJ because they are not typically imaged with MR imaging or because the unexposed bone does not raise the suspicion of BRONJ. In doubtful cases (i.e., ambivalent signal on T1- and T2-weighted images), signal changes in gingival region, inferior alveolar nerve, and neighboring soft-tissue MR imaging, not readily appreciated, even in the contrast-enhanced CT also due to metal artifacts that may obscure the lesions in CT, may suggest BRONJ (Fig. 6.10). The involvement in MRI may appear more extensive after contrast enhancement than in CT [9, 41], but imaging-based disease quantification should preferably encounter native T1- and T2-weighted findings though the latter usually overestimate the disease extent compared to intraoperative findings [9, 21] or offer no significant additional information for the resection margins [42]. Up to now and partly due to study design problems, there are no longitudinal studies reporting on the clinical fate of "silent" changes seen in CT or MRI not concordant to the classical BRONJ appearance.

In late stages or chronic cases, the reported signal intensity on T2-weighted images is also variable with predominating low T2 signal (or STIR-signal) indicating non-viable bone as reported in cases with uncontrollable pain unresponsive to conventional treatment before surgical resection [20]. Areas with unexposed bone may demonstrate increased, sometimes peripheral, signal intensity on T2-weighted or STIR images [6, 20] (Figs. 6.8 and 6.9). This signal intensity pattern implies probably a chronic osteomyelitis and is often accompanied by avid contrast enhancement. This corroborates the notion of the additive value of intravenous contrast for disease detection and quantification. However, contrast-enhanced MRI alone fails to distinguish between necrotic bone, osteomyelitis, and reactive signal changes of bone marrow secondary to surrounding inflammation of soft tissue. The bone marrow enhancement correlates with the degree of fatty marrow replacement and decreased signal intensity on T1-weighted images and typically spares the low T2 signal bony sequestrum (Figs. 6.8 and 6.9) [7, 9, 16]. In general, contrast enhancement may extend to the cortical bone, bone marrow, adjacent soft tissues

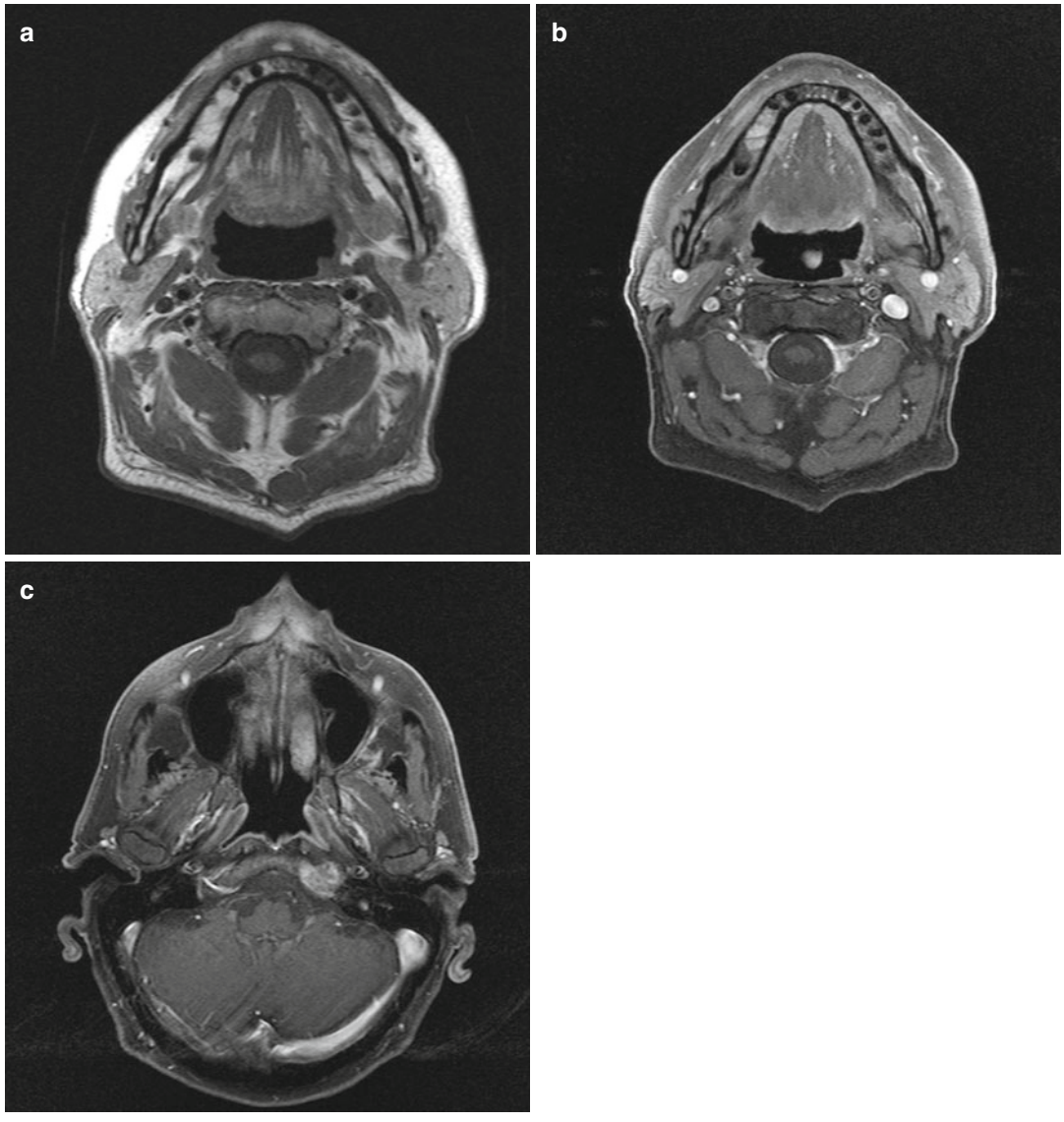

Fig. 6.7 (**a**–**c**) A 61-year-old woman with breast cancer and symptomatic osteonecrosis. Axial T1-weighted image (**a**) shows focal lesion of osteonecrosis in the left mandible as hypointense zone without cortical affection. After gadolinium administration and fat saturation (**b**), the lesion does not demonstrate significant enhancement. Adjacent fat-saturated, post-contrast T1-weighted MR image shows enhancing metastatic lesion in the left middle skull base (**c**)

(including mylohyoid ridge, buccinator muscle, orbicular muscle, and masticator space), paranasal sinuses, inferior alveolar and mandibular canal, and in the locoregional lymph nodes (Fig. 6.11). The commonly seen focal mass-like thickening of the adjacent soft tissue as well as cervical lymphadenopathy may clinically mimic neoplastic disease, either relapsing tumors or metastases (Fig. 6.11). The mass-like tissue changes are frequently located submandibular followed by the submandibular angle and jugulodigastric chains and should be encountered in the differential diagnosis [16, 37].

When we compare side-by-side the different imaging techniques, the overall detectability of BRONJ lesions in MR imaging is very high,

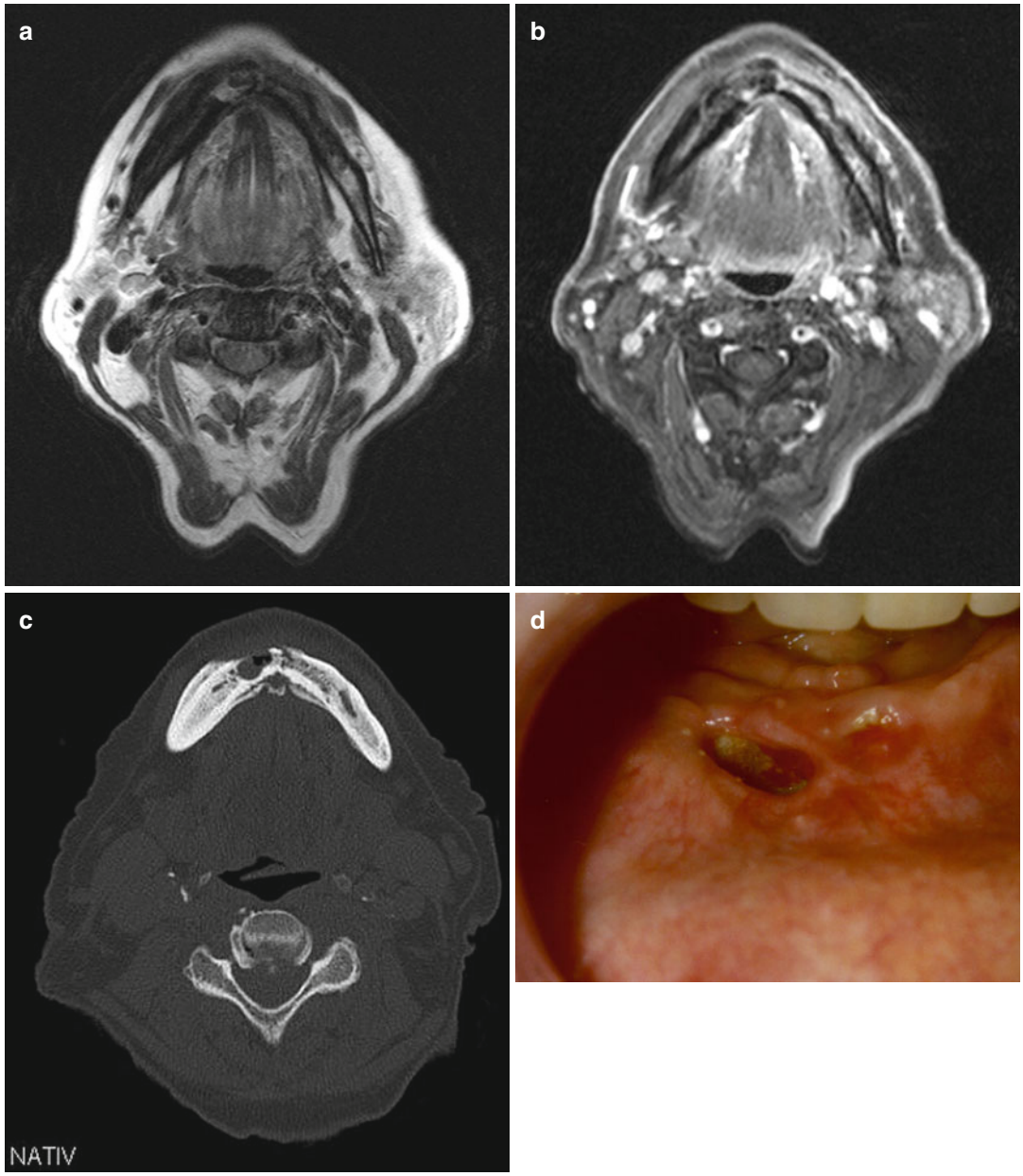

Fig. 6.8 (**a**–**d**) A 50-year-old woman with breast cancer. Axial T2-weighted image (**a**) shows pathologic mesial fracture in the mandible as well as decreased marrow signal intensity with cortical affection and hyperostosis on the right side, accompanied by soft-tissue changes in the labial and buccal premandibular region. The soft-tissue changes and the affected bone marrow, especially on the left side, show avid enhancement in fat-saturated T1-weighted image (**b**). The corresponding axial CT image (**c**) demonstrates cortical thickening, medullary sclerosis, pathologic fracture, and non-healing socket, the latter being also evident in the clinical examination (**d**)

justifying its application as a preoperative and monitoring tool [20]. However, a close correlation between intraoperative and MR imaging findings is not always evident [9, 21]. The sensitivity of MRI in identification of BRONJ is heavily dependent on the use of contrast enhancing MR sequences and should be encountered as high considering the identification of all the

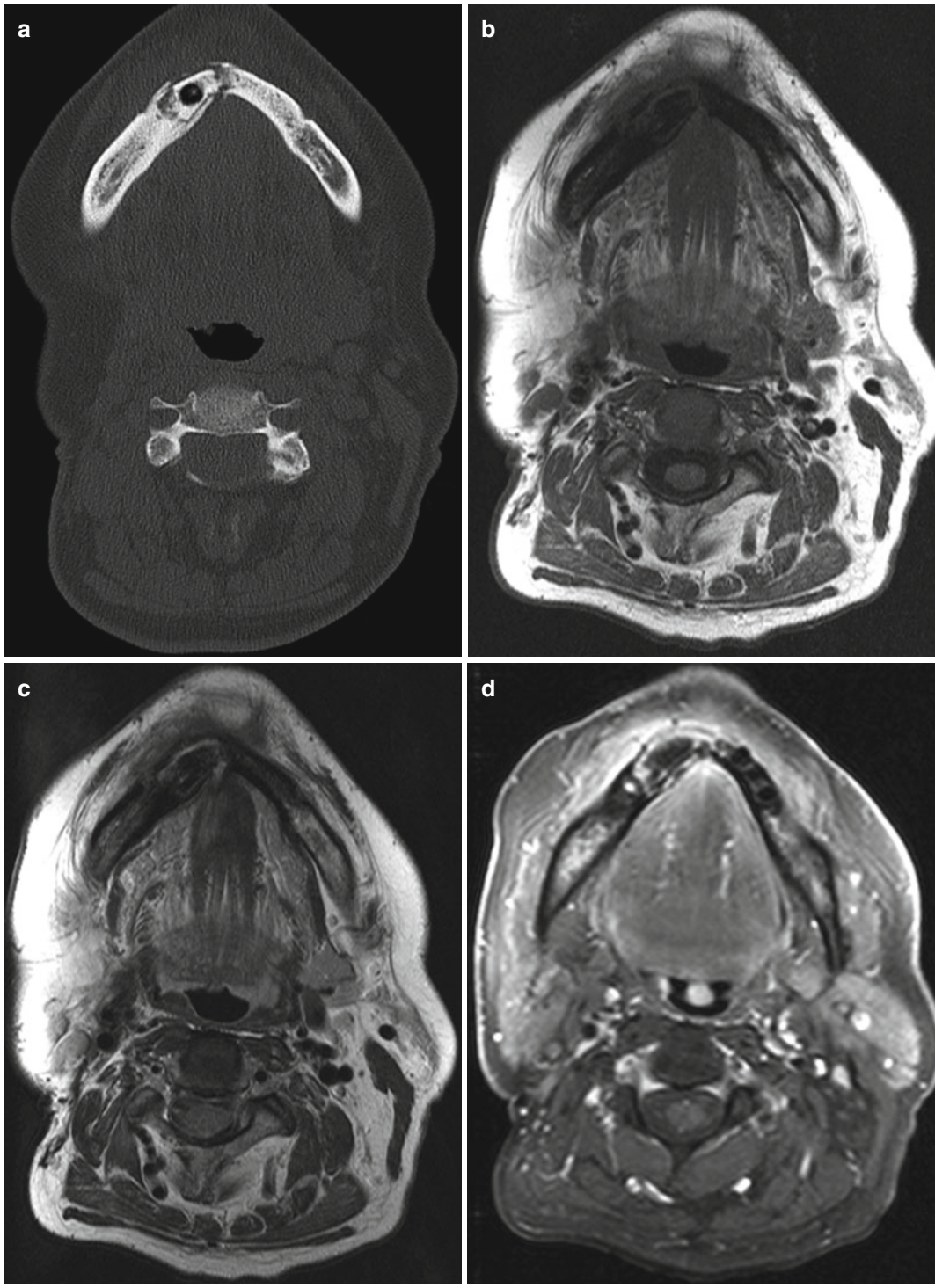

Fig. 6.9 (**a**–**d**) A 60-year-old male with prostate cancer. Axial CT image (**a**) shows bony sequestrum in the right mandibular body as well as medullar and cortical sclerosis on both sides. The corresponding unenhanced T1-weighted image (**b**) demonstrates the sclerotic lesions as areas with low signal intensity, whereas the T2-weighted image (**c**) shows intermediate signal intensity. The MR images reveal also soft-tissue changes in the labial and lingual adjacent tissue. The soft-tissue inflammation presents with avid enhancement in the fat-saturated, post-contrast T1-weighted image (**d**)

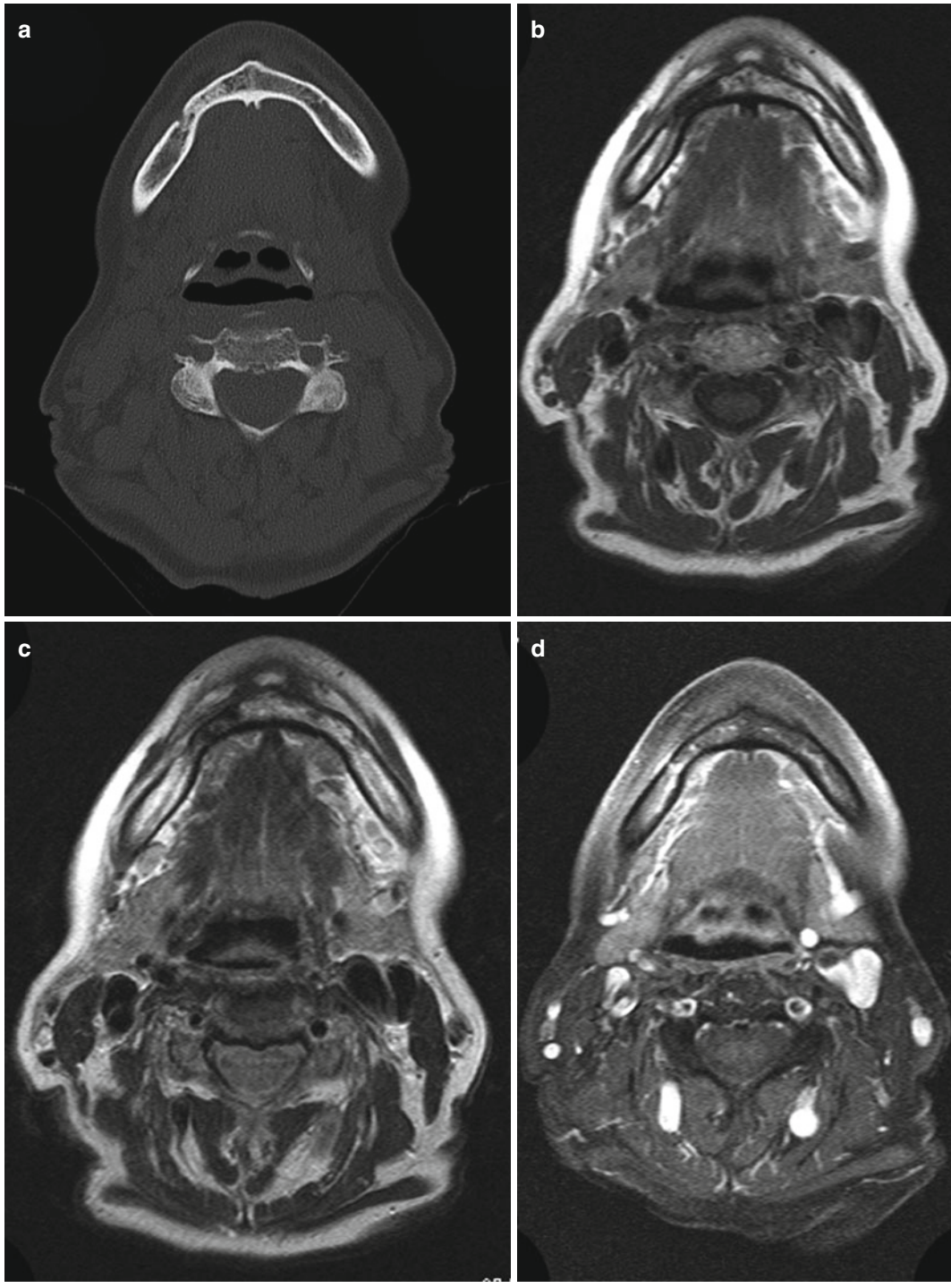

Fig. 6.10 (**a**–**d**) A 54-year-old woman with breast cancer and intermittent pain on the right mandible. Axial CT image (**a**) shows subtle focal sclerosis on the right mandible next to the mental foramen. The suspected area appears with low signal intensity on unenhanced T1-weighted (**b**) and T2-weighted (**c**) images, whereas it shows remarkable gadolinium enhancement on fat-suppressed, post-contrast T1-weighted image (**d**) the contrast enhancement seems to follow the right inferior alveolar canal; focal inflammation of the gingival tissue is also present

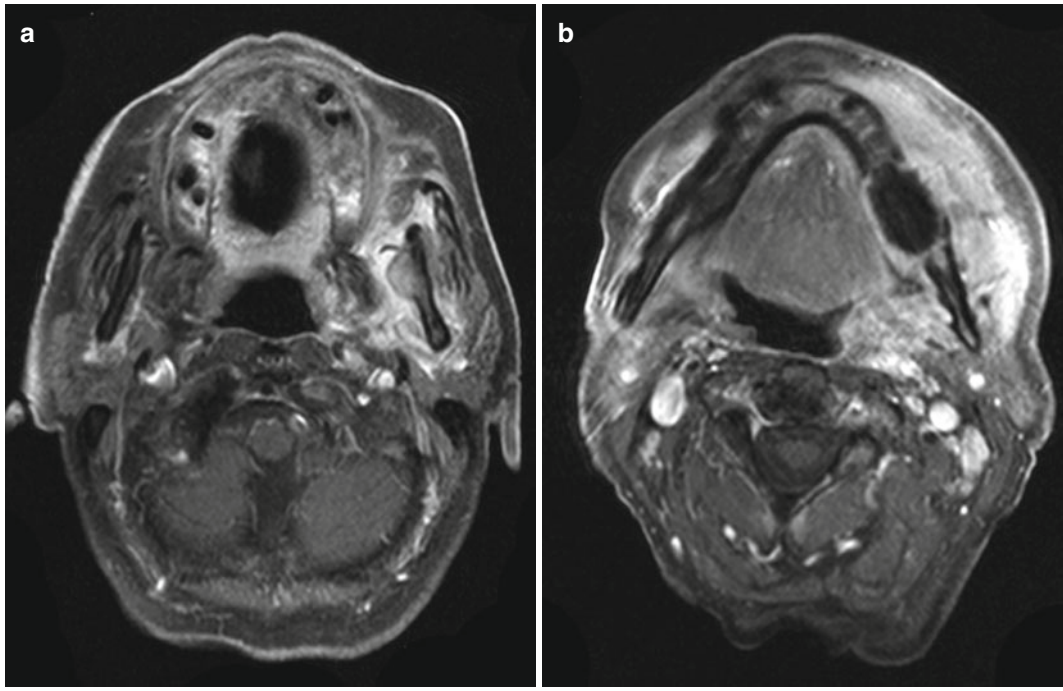

Fig. 6.11 (**a**–**b**) Fat-suppressed, post-contrast, T1-weighted MR imaging of a 67-year-old woman with multiple myeloma and BRONJ lesions on the maxilla and mandible. Axial image (**a**) demonstrates increased gadolinium uptake in the maxilla and left mandible as well as prominent enhancement of the soft tissues adjacent to the left mandibular ramus. There is fluid collection on the buccal side of the maxilla and on the mandibular foramen. The adjacent axial section at the level of the mandible (**b**) reveals the extensive inflammatory changes in the buccal region as well as in the oropharyngeal space and the tonsillar region on the left side. The bony marrow shows increased gadolinium uptake and the left mandible is fragmented with sequestration

symptomatic lesions and additional lesions not appreciated at clinical examination [37, 43].

Taken together, MRI may be advantageous over other imaging modalities in helping to exclude other possible diseases, delimiting the area of the lesion with bone and soft-tissue involvement, and guiding the therapeutic approach (i.e., debridement in intractable cases not responding to conservative treatment).

Nuclear Medicine Imaging Techniques

Functional imaging with bone scintigraphy, bone single-photon emission computed tomography (SPECT), positron emission tomography (PET), and combinations with computed tomography (SPECT/CT, PET/CT) finally complete the imaging spectrum of MRONJ imaging. While radiographs, CT, and MRI are able to display osteonecrotic pattern, they have low specificity for BRONJ lesions [8, 16, 44]. Reliable detection of early BRONJ lesions and assessment of the extent of a lesion are limited so far. Therefore, functional nuclear medicine techniques were investigated as well in the context of BRONJ imaging.

Bone scintigraphy was identified to present with alterations of radionuclide uptake in BRONJ lesions [6, 45, 46]. 99Tcm-MDP uptake is generally influenced by blood flow and osteoblastic metabolism. Chinadussi et al. reported decreased 99Tcm-MDP uptake in early stages when vascularization is lowered and increased uptake in later stages due to higher osteoblast activity in advanced disease [6]. SPECT confirmed the presence of increased uptake, and it was concluded

that scintigraphy might be used as a screening test to detect subclinical osteonecrosis in patients receiving bisphosphonates [6]. A drawback of conventional bone scintigraphy and SPECT however is the low spatial resolution and a certain lack in anatomical information. Hybrid SPECT/CT can improve the accuracy of scintigraphy because SPECT/CT provides a functional–anatomical correlation. Accordingly, it was reported that SPECT/CT increased the accuracy of conventional imaging and differentiation between the necrosis and adjacent viable bone became possible [46].

A comparison between two functional imaging techniques, characterized, on the one hand, by a tracer showing oncotropic properties, such as Tc99m-sestamibi, and, on the other hand, a tracer taken up by inflammation such as FDG-PET, was reported to support differentiation between BRONJ lesions and myeloma osteolysis in a preliminary report [45, 47].

Further studies demonstrated focal enhancement on PET scans at sites of BRONJ lesions [43, 44, 48]. PET enhancement is related to vascularization and hypermetabolism. Therefore, uptake in BRONJ lesions may be due to hypermetabolism caused by superimposing infection or healing response and may not be caused by the necrosis itself [44]. In a present study based on 46 PET scans, it was shown that enhancement on a PET scan is not a reliable indicator of BRONJ and that a non-enhancing scan does not necessarily exclude the disease. In conclusion, the results did not support a routine use in the diagnostic of BRONJ [44]. However, Wilde et al. suggested that PET might serve as an option for visualizing the severity of BRONJ and could be valuable for evaluation of treatment effects. Combined PET/CT techniques may further improve the diagnosis of BRONJ by combining functional and anatomical information [48].

While scintigraphy, SPECT, and PET are not useful for metric analysis of BRONJ [9], combined PET/CT was assessed to detect more extensive involvement of BRONJ compared with panoramic views from CBCT and clinical examinations, although, comparable to contrast-enhanced MRI, the real dimension of a lesion may be overestimated [21].

Conclusions

At present, panoramic radiographs can be considered as a primary modality for MRONJ imaging. In clinical routine, CT and CBCT are widely used to gain further three-dimensional information of the extent of osteonecrosis and to clarify if there are any further findings like pathological fractures or signs of sinusitis. So far, there is no final evidence that MRI is superior to CT in order to display the extent of the lesion or to detect early stages of BRONJ. Anyway, it seems like CT and MRI offer a wide spectrum of findings but those are often not very specific. Nuclear medicine tomographic imaging techniques may be useful in detecting early stages and monitoring the disease; however, they cannot be regarded as standard in MRONJ imaging at the moment.

References

1. Ruggiero SL, Dodson TB, Assael LA, Landesberg R, Marx RE, Mehrotra B. American Association of Oral and Maxillofacial Surgeons position paper on bisphosphonate-related osteonecrosis of the jaws–2009 update. J Oral Maxillofac Surg. 2009;67(5 Suppl):2–12. PubMed PMID: 19371809. Epub 2009/04/25. eng.
2. Lo JC, O'Ryan FS, Gordon NP, Yang J, Hui RL, Martin D, et al. Predicting Risk of Osteonecrosis of the Jaw with Oral Bisphosphonate Exposure (PROBE) Investigators. Prevalence of osteonecrosis of the jaw in patients with oral bisphosphonate exposure. J Oral Maxillofac Surg. 2010;68(2):243–53. PubMed PMID: 19772941. Epub 2009/09/24. eng.
3. Hutchinson M, O'Ryan F, Chavez V, Lathon PV, Sanchez G, Hatcher DC, et al. Radiographic findings in bisphosphonate-treated patients with stage 0 disease in the absence of bone exposure. J Oral Maxillofac Surg. 2010;68(9):2232–40. PubMed PMID: 20728032. eng.
4. Rocha GC, Jaguar GC, Moreira CR, Neves EG, Fonseca FP, Pedreira EN. Radiographic evaluation of maxillofacial region in oncology patients treated with bisphosphonates. Oral Surg Oral Med Oral Pathol Oral Radiol. 2012;114(5 Suppl):S19–25. PubMed PMID: 23083951. Epub 2012/02/18. eng.
5. Arce K, Assael LA, Weissman JL, Markiewicz MR. Imaging findings in bisphosphonate-related osteonecrosis of jaws. J Oral Maxillofac Surg. 2009;67(5 Suppl):75–84. PubMed PMID: 19371818. eng.
6. Chiandussi S, Biasotto M, Cavalli F, Cova MA, Di Learda R. Clinical and diagnostic imaging of bisphosphonate-associated osteonecrosis of the jaws.

Dentomaxillofac Radiol. 2006;35:236–43. PubMed PMID: 16798918. eng.
7. Morag Y, Morag-Hezroni M, Jamadar DA, Ward BB, Jacobson JA, Zwetchkenbaum SR, et al. Bisphosphonate-related osteonecrosis of the jaw: a pictorial review. Radiographics. 2009;29(7):1971–84. PubMed PMID: 19926757. eng.
8. Popovic KS, Kocar M. Imaging findings in bisphosphonate-induced osteonecrosis of the jaws. Radiol Oncol. 2010;44(4):215–9. PubMed PMID: 22933918. Epub 2010/06/24. eng.
9. Stockmann P, Hinkmann FM, Lell MM, Fenner M, Vairaktaris E, Neukam FW, Nkenke E. Panoramic radiograph, computed tomography or magnetic resonance imaging. Which imaging technique should be preferred in bisphosphonate-associated osteonecrosis of the jaw? A prospective clinical study. Clin Oral Investig. 2010;14(3):311–7.
10. Wilde F, Heufelder M, Lorenz K, Liese S, Liese J, Helmrich J, et al. Prevalence of cone beam computed tomography imaging findings according to the clinical stage of bisphosphonate-related osteonecrosis of the jaw. Oral Surg Oral Med Oral Pathol Oral Radiol. 2012;114(6):804–11. PMID: 23159120. eng.
11. Phal PM, Myall RW, Assael LA, Weissman JL. Imaging findings of bisphosphonate-associated osteonecrosis of the jaws. AJNR Am J Neuroradiol. 2007;28(6):1139–45. PubMed PMID: 17569974. eng.
12. Torres SR, Chen CS, Leroux BG, Lee PP, Hollender LG, Santos EC, Drew SP, Hung KC, Schubert MM. Mandibular cortical bone evaluation on cone beam computed tomography images of patients with bisphosphonate-related osteonecrosis of the jaw. Oral Surg Oral Med Oral Pathol Oral Radiol. 2012;113(5):695–703. PubMed PMID: 22668629. Epub 2012/04/12. eng.
13. Groetz KA, Al-Nawas B. Persisting alveolar sockets—a radio- logic symptom of BP-ONJ? J Oral Maxillofac Surg. 2006;64:1571–2. PubMedPMID: 16982320. eng.
14. Durie BG, Katz M, Crowley J. Osteonecrosis of the jaw and bisphosphonates. N Engl J Med. 2005;353(1):99–102; discussion 99–102. PubMed PMID: 16000365. eng.
15. Hewitt C, Farah CS. Bisphosphonate-related osteonecrosis of the jaws: a comprehensive review. J Oral Pathol Med. 2007;36(6):319–28. PubMed PMID: 17559492. eng.
16. Bisdas S, Chambron Pinho N, Smolarz A, Sader R, Vogl TJ, Mack MG. Bisphosphonate-induced osteonecrosis of the jaws: CT and MRI spectrum of findings in 32 patients. Clin Radiol. 2008;63(1):71–7. PubMed PMID: 18068792. Epub 2007 Oct 22. eng.
17. Bianchi SD, Scoletta M, Cassione FB, Migliaretti G, Mozzati M. Computerized tomographic findings in bisphosphonate-associated osteonecrosis of the jaw in patients with cancer. Oral Surg Oral Med Oral Pathol Oral Radiol Endod. 2007;104(2):249–58. PMID: 17560140. Epub 2007/06/07.
18. Gill SB, Valencia MP, Sabino ML, Heideman GM, Michel MA. Bisphosphonate-related osteonecrosis of the mandible and maxilla: clinical and imaging features. J Comput Assist Tomogr. 2009;33(3):449–54. PubMed PMID: 19478642. eng.
19. Marx RE, Sawatari Y, Fortin M, Broumand V. Bisphosphonate-induced exposed bone (osteonecrosis/osteopetrosis) of the jaws: risk factors, recognition, prevention, and treatment. J Oral Maxillofac Surg. 2005;63(11):1567–75. PubMed PMID: 16243172. eng.
20. Bedogni A, Blandamura S, Lokmic Z, Palumbo C, Ragazzo M, Ferrari F, et al. Bisphosphonate-associated jawbone osteonecrosis: a correlation between imaging techniques and histopathology. Oral Surg Oral Med Oral Pathol Oral Radiol Endod. 2008;105(3):358–64. PubMed PMID: 18280968. eng.
21. Guggenberger R, Fischer DR, Metzler P, Andreisek G, Nanz D, Jacobsen C, et al. Bisphosphonate-induced osteonecrosis of the jaw: comparison of disease extent on contrast-enhanced MR imaging, [18F] fluoride PET/CT, and conebeam CT imaging. AJNR Am J Neuroradiol. 2013;34(6):1242–7. PMID: 23221951. Epub 2012/12/6. eng.
22. Assaf AT, Zrnc TA, Riecke B, Wikner J, Zustin J, Friedrich RE, et al. Intraoperative efficiency of fluorescence imaging by Visually Enhanced Lesion Scope (VELscope) in patients with bisphosphonate related osteonecrosis of the jaw (BRONJ). J Craniomaxillofac Surg. 2014;42(5):157–64. PubMed PMID: 24011463. eng.
23. Pautke C, Bauer F, Otto S, Tischer T, Steiner T, Weitz J, et al. Fluorescence-guided bone resection in bisphosphonate-related osteonecrosis of the jaws: first clinical results of a prospective pilot study. J Oral Maxillofac Surg. 2011;69(1):84–91. PubMed PMID: 20971542. Epub 2010/10/26. eng.
24. Elad S, Gomori MJ, Ben-Ami N, Friedlander-Barenboim S, Regev E, Lazarovici TS, Yarom N. Bisphosphonate-related osteonecrosis of the jaw: clinical correlations with computerized tomography presentation. Clin Oral Investig. 2010;14(1):43–50. PubMed PMID: 19603201. Epub 2009/07/15. eng.
25. Allen MR, Ruggiero SL. Higher bone matrix density exists in only a subset of patients with bisphosphonate-related osteonecrosis of the jaw. J Oral Maxillofac Surg. 2009;67(7):1373–7. PubMed PMID: 19531405. eng.
26. De Vos W, Casselman J, Swennen GR. Cone-beam computerized tomography (CBCT) imaging of the oral and maxillofacial region: a systematic review of the literature. Int J Oral Maxillofac Surg. 2009;38:609–25. PubMed PMID: 19464146. Epub 2009/05/21. eng.
27. Loubele M, Bogaerts R, Van Dijck E, et al. Comparison between effective radiation dose of CBCT and MSCT scanners for dentomaxillofacial applications. Eur J Radiol. 2009;71:461–8. PubMed PMID: 18639404. Epub 2008/07/18. eng.
28. Schulze D, Heiland M, Thurmann H, Adam G. Radiation exposure during midfacial imaging using 4- and 16-slice computed tomography, cone beam computed tomography systems and conventional radiography. Dentomaxillofac Radiol. 2004;33:83–6. PubMed PMID: 15313998. eng.
29. Barragan-Adjemian C, Lausten L, Ang DB, Johnson M, Katz J, Bonewald LF. Bisphosphonate-related osteonecrosis of the jaw: model and diagnosis with cone beam computerized tomography. Cells Tissues

Organs. 2009;189:284–8. Pubmed PMID: 18703870. Epub 2008/08/15. eng.
30. Fleisher KE, Doty S, Kottal S, Phelan J, Norman RG, Glickman RS. Tetracycline-guided debridement and cone beam computed tomography for the treatment of bisphosphonate-related osteonecrosis of the jaw: a technical note. J Oral Maxillofac Surg. 2008;66(12): 2646–53. PubMed PMID: 19022151. Epub 2008/11/22. eng.
31. Singer SR, Mupparapu M. Plain film and CBCT findings in a case of bisphosphonate-related osteonecrosis of the jaw. Quintessence Int. 2009;40:163–5. PubMed PMID: 19169448. eng.
32. Treister NS, Friedland B, Woo SB. Use of cone-beam computerized tomography for evaluation of bisphosphonate-associated osteonecrosis of the jaws. Oral Surg Oral Med Oral Pathol Oral Radiol Endod. 2010;109(5):753–64. PubMed PMID: 20303301. Epub 2010/05/29. eng.
33. Olutayo J, Olubanwo Agbaje J, Jacobs R, Verhaeghe V, Vande Velde F, Vinckier F. Bisphosphonate-related osteonecrosis of the jaw bone: radiological pattern and the potential role of CBCT in early diagnosis. J Oral Maxillofac Res. 2010;1:e3. Available at http://www.ejomr.org/JOMR/archives/2010/2/e3/e3ht.htm.
34. Kalender WA, Kyriakou Y. Flat-detector computed tomography (FD-CT). Eur Radiol. 2007;17:2767–79. PubMed PMID: 17587058. Epub 2007/06/23. eng.
35. Mast G, Otto S, Mucke T, Schreyer C, Bissinger O, Kolk A, et al. Incidence of maxillary sinusitis and oro-antral fistulae in bisphosphonate-related osteonecrosis of the jaw. J Craniomaxillofac Surg. 2012;40(7): 568–71. PubMed PMID: 22118926. Epub 2011/11/29. eng.
36. Maurer P, Sandulescu T, Kriwalsky MS, Rashad A, Hollstein S, Stricker I, et al. Bisphosphonate-related osteonecrosis of the maxilla and sinusitis maxillaris. Int J Oral Maxillofac Surg. 2011;40(3):285–91. PubMed PMID: 21163624. Epub 2010/12/15.
37. Garcia-Ferrer L, Bagan JV, Martinez-Sanjuan V, Hernandez-Bazan S, Garcia R, Jimenez-Soriano Y, et al. MRI of mandibular osteonecrosis secondary to bisphosphonates. AJR Am J Roentgenol. 2008; 190(4):949–55. PubMed PMID: 18356441. eng.
38. Takao M, Sugano N, Nishii T, Sakai T, Nakamura N, Yoshikawa H. Different magnetic resonance imaging features in two types of nontraumatic rabbit osteonecrosis models. Magnetic resonance imaging. Magn Reson Imaging. 2009;27(2):233–9.
39. Fatterpekar GM, Emmrich JV, Eloy JA, Aggarwal A. Bone-within-bone appearance: a red flag for biphosphonate-associated osteonecrosis of the jaw. J Comput Assist Tomogr. 2011;35(5):553–6. PubMed PMID: 21926848. eng.
40. Khosla S, Burr D, Cauley J, Dempster DW, Ebeling PR, Felsenberg D, et al. Bisphosphonate-associated osteonecrosis of the jaw: report of a task force of the American Society for Bone and Mineral Research. J Bone Miner Res. 2007;22(10):1479–91. PubMed PMID: 17663640. eng.
41. Fox MG, Stephens T, Jarjour WN, Anderson MW, Kimpel DL. Contrast-enhanced magnetic resonance imaging positively impacts the management of some patients with rheumatoid arthritis or suspected RA. J Clin Rheumatol. 2012;18(1):15–22. PubMed PMID: 22157267. eng.
42. Wutzl A, Eisenmenger G, Hoffmann M, Czerny C, Moser D, Pietschmann P, et al. Osteonecrosis of the jaws and bisphosphonate treatment in cancer patients. Wien Klin Wochenschr. 2006;118(15–16):473–8. PubMed PMID: 16957978. eng.
43. Raje N, Woo SB, Hande K, Yap JT, Richardson PG, Vallet S, et al. Clinical, radiographic, and biochemical characterization of multiple myeloma patients with osteonecrosis of the jaw. Clin Cancer Res. 2008;14(8):2387–95. PubMed PMID: 18413829. eng.
44. Belcher R, Boyette J, Pierson T, Siegel E, Bartel TB, Aniasse E, et al. What is the role of positron emission tomography in osteonecrosis of the jaws? J Oral Maxillofac Surg. 2014;72(2):306–10. doi:10.1016/j.joms.2013.07.038. pii: S0278-2391(13)00950-6. PubMed PMID: 24075237. eng.
45. Catalano L, Del Vecchio S, Petruzziello F, Fonti R, Salvatore B, Martorelli C, et al. Sestamibi and FDG-PET scans to support diagnosis of jaw osteonecrosis. Ann Hematol. 2007;86(6):415–23. PubMed PMID: 17285274. Epub 2007 Feb 7. eng.
46. Dore F, Filippi L, Biasotto M, Chiandussi S, Cavalli F, Di Lenarda R. Bone scintigraphy and SPECT/CT of bisphosphonate-induced osteonecrosis of the jaw. J Nucl Med. 2009;50(1):30–5. PubMed PMID: 19091894. eng.
47. Fabbricini R, Catalano L, Pace L, Del Vecchio S, Fonti R, Salvatore M, Rotoli B. Bone scintigraphy and SPECT/CT in bisphosphonate-induced osteonecrosis of the jaw. J Nucl Med. 2009;50(8):1385; author reply 1385. Epub 2009/07/17. PubMed PMID: 19617329.
48. Wilde F, Steinhoff K, Frerich B, Schulz T, Winter K, Hemprich A, et al. Positron-emission tomography imaging in the diagnosis of bisphosphonate-related osteonecrosis of the jaw. Oral Surg Oral Med Oral Pathol Oral Radiol Endod. 2009;107(3):412–9. PubMed PMID: 19121962. Epub 2009/01/04. eng.